

3 Xinyuan Wen¹, Dianfeng Liu^{1,2*}, Mingli Qiu¹ and Yinjie Wang¹

⁴ ¹ School of Resources and Environmental Sciences, Wuhan University, Wuhan, PR China.

² Key Laboratory of Digital Cartography and Land Information Application Engineering, Ministry of Natural Resources, Wuhan, PR China.

⁷ *Corresponding author: Dianfeng Liu (liudianfeng@whu.edu.cn)

8 Key Points:

- Statistical model and spatial simulation model are combined to estimate maize yield
 - Synergistic effect of climatic and land-use changes on maize yield is examined
 - Yield gaps among counties necessitates differentiated policies of agricultural production

13 Abstract

14 Yield forecasting can give early warning of food risks and provide theoretical support for food
15 security planning. Climate change and land use change directly influence the regional yield and
16 planting area of maize, but few existing studies have examined their synergistic impact on maize
17 production. In this study, we combine system dynamic (SD), the future land use simulation
18 (FLUS) and a statistical crop model to predict future maize yield variation in response to climate
19 change and land use change. Specifically, SD predicts the future land use demand, FLUS
20 simulates future spatial land use patterns, and a statistical maize yield model based on regression
21 analysis is utilized to adjust the per hectare maize yield under four representative concentration
22 pathways (RCPs). A phaeozem region in central Jilin Province of China is taken as a case study.
23 The results show that the future land use pattern will significantly change from 2030 to 2050.
24 Although the cultivated land is likely to reduce by 862.84 km², the total maize yield in 2050 will
25 increase under all four RCP scenarios due to the promotion of per hectare maize yield. RCP4.5
26 will be more beneficial to maize production than other scenarios, with a doubled total yield in
27 2050. Notably, the yield gap between different counties will be further widened, which
28 necessitates the differentiated policies of agricultural production and farmland protection, e.g.,
29 strengthening cultivated land protection and crop management in low-yield areas, as well as
30 taking adaptation and mitigation measures to coordinate climate change and crop production.

31

32 Plain Language Summary

33 We propose a simulation framework based on the integration of system dynamic (SD), future
34 land use simulation model (FLUS) and a statistical maize yield model. And we predict the effects
35 of future climate and land use change under different representative concentration pathways
36 (RCPs) on rain-fed maize yield in a typical black-soil region of China, Jilin Province. We find
37 that the cultivated land area will decrease, but the total maize yield will increase due to the
38 promotion of maize yield per hectare. At the same time, the spatial heterogeneity of regional
39 maize production will be intensified.

40 Keywords

41 Maize yield; land use simulation; RCP scenarios; climatic and land-use changes; models

42 1 Introduction

43 Agriculture plays a vital role in food security, poverty elimination and sustainable
 44 development ([Loboguerrero et al., 2019](#)). With the remarkable growth of the global population,
 45 agricultural production has faced a significant challenge in meeting the increasing food demand
 46 and varying diet structure of human beings. Moreover, farmland loss and degradation caused by
 47 urban expansion and economic development have exacerbated this situation ([Vermeulen et al.,](#)
 48 [2012](#)). In this context, forecasting food production can give an early warning of food risk and
 49 support agricultural land use activities and the corresponding policy making.

50 The existing yield prediction methods can be categorized into statistical models and
 51 process-based models. The traditional statistical models have been commonly employed to
 52 forecast seasonal variations of crop yield, e.g., linear and non-linear regression analysis and their
 53 integration with principal component analysis. Currently, machine learning approaches, e.g.,
 54 random forest ([Sakamoto, 2020](#)), XGBoost, long-short-term memory (LSTM), and convolutional
 55 neural network (CNN), have received more and more attention due to their ability to describe
 56 complicated relationships of crop production and the driving forces ([Hengl et al., 2017](#); [Kang et](#)
 57 [al., 2020](#); [Leng and Hall, 2020](#); [Poornima and Pushpalatha, 2019](#); [Yang et al., 2019](#); [Zhong et al.,](#)
 58 [2019](#)). These statistical models can relate historical yield data with the agrometeorological
 59 variables, for example, march temperature difference, daily relative humidity changes, sunshine
 60 hours, and the remote sensing-based variables ([Banakara et al., 2019](#); [Camberlin and Diop, 1999](#),
 61 [Giri et al., 2017](#); [Sharma et al., 2017](#)), such as Normalized Difference Vegetation Index ([Peralta](#)
 62 [et al., 2016](#)), Vegetation Condition Index ([Kowalik et al., 2014](#)), and Vegetation Health Index
 63 ([Wang et al., 2010](#)).

64 Process-based crop models employ integrated mathematical methods to describe crop
 65 growth status driven by climate, nutrient and water cycling, soil properties and agricultural
 66 management practices ([Basso et al., 2016](#)). This type of models includes CERES-Millet, EARS-
 67 CGS, PUTU, WOFOST and SWAP ([Manatsa et al., 2011](#); [Roebeling et al., 2004](#); [Rojas, 2007](#);
 68 [Tripathy et al., 2013](#)), which have been applied to maize, wheat, barley, and millet prediction.
 69 Although these models have been proven efficient in practice, they still suffer from significant
 70 uncertainties because of complex parameters calibration and initialization ([Kolotii et al., 2015](#)).
 71 For example, a number of these models will be calibrated using genetic information of plants that

72 is hardly quantified. In contrast, statistical models allow us to capture essential processes that
73 may be overlooked in the process model, including the impact of extreme temperatures on
74 canopy transpiration and photosynthesis and the damage to crops caused by weather, pests, and
75 diseases ([Urban et al., 2012](#)). Therefore, this study adjusted a statistical model to predict maize
76 yield per hectare instead of a process-based crop model.

77 Climate and land use change have been regarded as two worldwide influencing factors of
78 maize production ([Basso and Liu, 2019](#)). Climate change affects crop growth by changing
79 temperature, precipitation, CO₂, nitrogen, and other critical ecological factors, during the
80 growing season. Land use change analysis can improve yield forecasts' accuracy by identifying
81 the chop's changed planting areas ([Vancutsem et al., 2013](#)). However, a better understanding of
82 the synergistic effect of climate change and land use change on maize yield in a spatially explicit
83 way is still lacking at present. Combining statistical models and spatial land use simulation
84 models have been proven promising to address this issue. Land use simulation approaches
85 originated from cellular automata enable us to project changes in quantity and spatial pattern of
86 agricultural land, and incorporate the effect of land use change into the crop yield estimation
87 ([Akpoti et al., 2019](#); [Liu et al., 2017](#)). Moreover, these simulation models can be equipped with
88 various complex approaches, e.g., neural network, multi-agent system, and multinomial logistic
89 regression, to pursue better simulation performance ([Basse et al., 2014](#); [Mustafa et al., 2018](#);
90 [Yeldan et al., 2012](#)). Due to the flexible model framework, numerous driving factors can also be
91 incorporated into maize yields, like urbanization, agricultural machinery advancement, and
92 population economic growth, etc. ([Abate and Kuang, 2021](#); [Takeshima et al., 2013](#); [Yu et al.,
93 2020](#); [Zhang et al., 2017b](#)).

94 We demonstrated a new crop prediction framework based on the integration of a
95 statistical crop yield approach and a spatial land use simulation model, and examined the
96 synergistic effects of climate change and land use change on maize yields. Further, we designed
97 four future scenarios based on representative concentration paths (RCPs) to examine the direct
98 effects of climate change and socio-economic development on maize yield per hectare. We
99 conducted a case study in the phaeozem region of central Jilin Province, China, and validated the
100 proposed model. Our work is expected to provide a generic framework for the spatially explicit
101 forecast of maize yield.

102 **2 Materials and Methods**103 **2.1 Study area**

104 A phaeozem region in central Jilin Province of China was selected as the study area,
105 consisting of Changchun, Jilin, Siping, Liaoyuan, and Tonghua City (**Figure 1**). This region is
106 located in the major golden maize belts across the world, and plays an irreplaceable role in
107 national food security as one of the primary grain production bases and commodity grain export
108 bases in China ([Asseng et al., 2013](#); [Li et al., 2020](#)). The rain-fed maize system was selected as
109 the research object to eliminate the effect of irrigation on crop yield ([Urban et al., 2012](#)).

110 The region features a short growing season of maize from May to September ([Feng et al.,](#)
111 [2021](#); [Jiang et al., 2021](#); [Yang et al., 2007](#)). Over the past 50 years, the average annual
112 temperature has increased significantly by 0.38°C per decade, precipitation has decreased
113 slightly, and droughts and floods have become more frequent ([Liu et al., 2009](#); [Yin et al., 2016](#)).
114 Climate change will directly affect maize production. Existing studies have also shown that
115 climate change has an indirect impact on land use ([Pan et al., 2020](#); [Yang et al., 2020](#)). Therefore,
116 it is necessary to assess the future impact of climate change and land use change on maize yields
117 to support the decision-making of agricultural production.

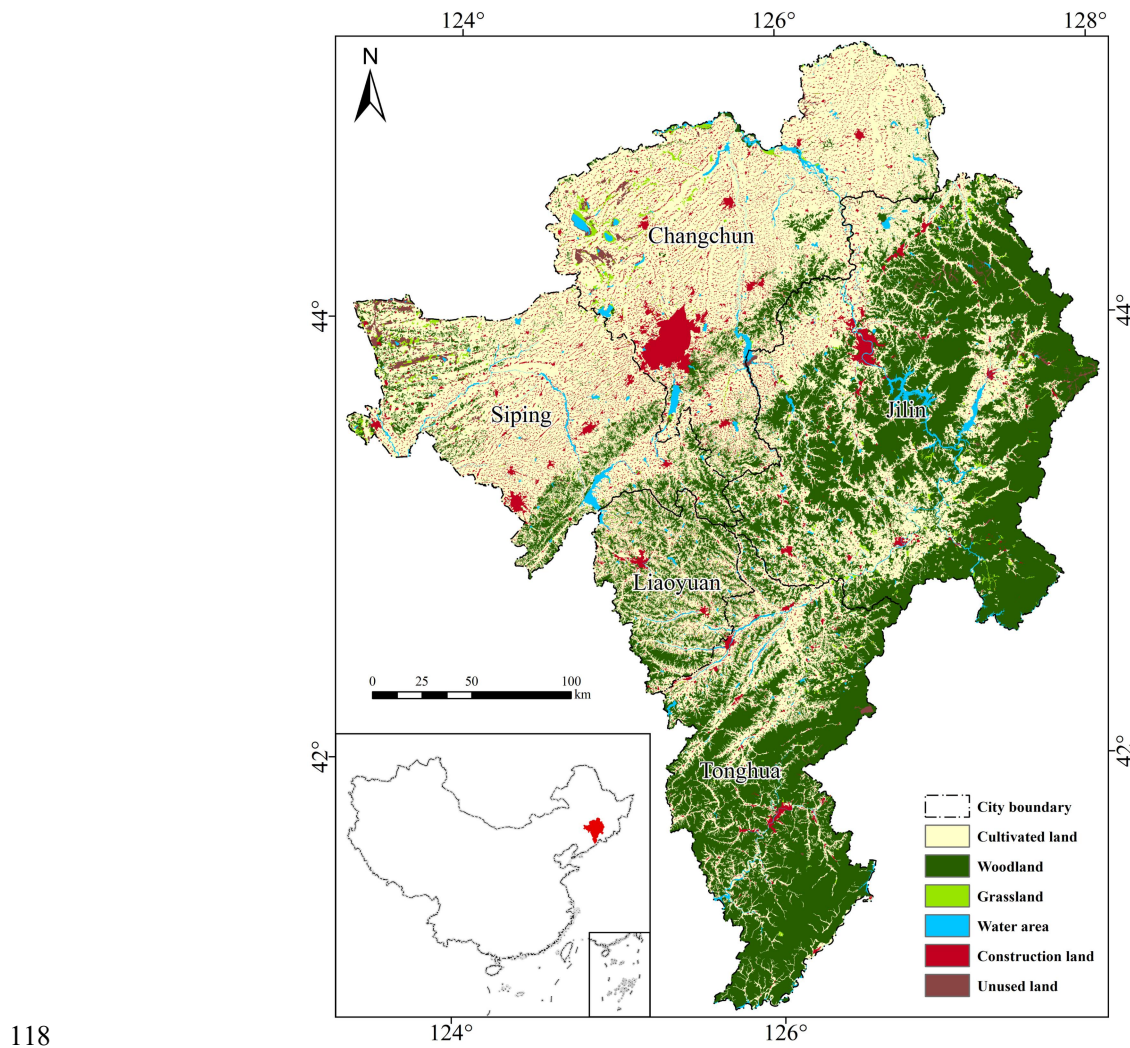


Figure 1. Location of the Study Area (background: empirical land use map in 2015).

2.2 Data source

The data collected in this study includes climate data, land use maps, socio-economic data and geographical information. Future climate data, i.e., precipitation and surface temperatures, were collected from WDCC (<https://cera-www.dkrz.de>), which were generated using general circulation modelthe Beijing Climate Center Climate System Model version 1.1 m (BCC_CSM1.1 m)([Knutti, 2014](#)). The data are at a T106 horizontal resolution ($1.125^\circ \times 1.125^\circ$) ([Liu et al., 2021](#); [Wu et al., 2010](#)), and have been widely used to explore maize, wheat and other grain planting systems in northeast China ([Gao et al., 2020](#); [He et al., 2018](#); [Jiang et al., 2021](#)). Meanwhile, a time series of historical climate data was downloaded from the China Meteorological Data Network (<http://data.cma.cn>).

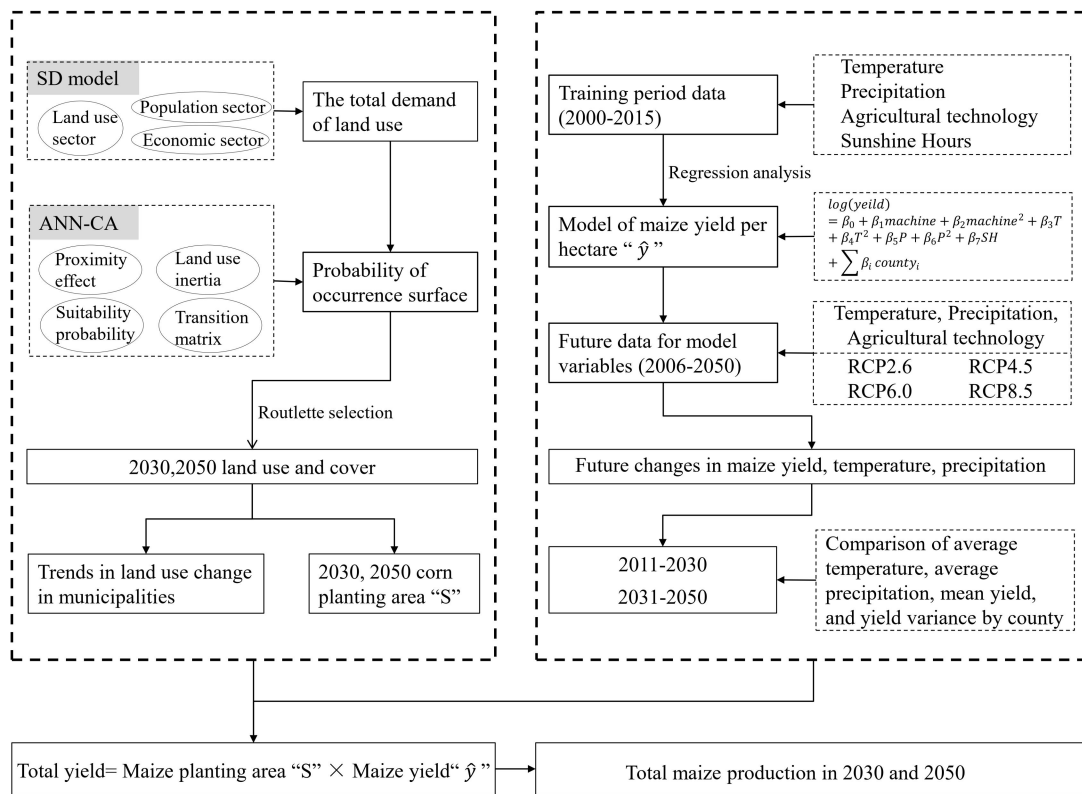
130 Empirical land use maps in 2000, 2005, 2010 and 2015 were derived from the Chinese
 131 Academy of Sciences (CAS; <http://www.resdc.cn>), categorized into six land use/cover types:
 132 cultivated land, woodland, grassland, construction land, unused land and water area([Ning et al.,](#)
 133 [2018](#)). Socio-economic data, including urban/rural population, agriculture production, forestry,
 134 animal husbandry and fishery, were obtained from the Statistical Yearbook of Jilin Province
 135 (2000-2015). The raster datasets of population density and GDP([Xinliang, 2017a, b](#)), and other
 136 geographic maps, including administrative boundaries, roads and railways, were derived from
 137 the Chinese Academy of Sciences database. On the ArcGIS 10.5 platform, all spatial data were
 138 converted into raster maps at a spatial resolution of 30m. See **Table 1** for detailed data
 139 information.

140 **Table 1**141 *Research data and sources*

Data	Data type	Temporal coverage	Source
Expenditure and production value of agriculture, forestry, animal husbandry and fishery	Excel	2000-2015	Jilin Province Statistical Yearbook
Total mechanical power, total grain production			
The proportion of urban population, total urban and rural population			
Science and technology expenditure			
County-level maize yield data			
Historical climate data	Excel	2000-2015	http://data.cma.cn/
Annual average precipitation and annual average temperature	NetCDF	2006-2100	https://cera-www.dkrz.de
Land use map	TIFF	2000-2015	http://data.casearth.cn/
GDP spatial distribution		2000, 2015	http://www.resdc.cn/
Spatial distribution of population density			
Digital Elevation Model (DEM)			
Road network	shapefile		https://www.openstreetmap.org/
Administrative boundary	shapefile	2015	http://www.resdc.cn/

143 **3 Methods**144 **3.1 Integrated assessment framework**

145 To examine the effect of climate change and land use changes on regional maize yield,
 146 we proposed an analytical framework based on the integration of system dynamics (SD), cellular
 147 automata (CA) and a statistical maize yield model (**Figure 2**). The SD projects land use demands
 148 from a top-down perspective based on socio-economic development and policy planning. The
 149 CA simulates spatial land use patterns from a bottom-up perspective. The integration of SD and
 150 CA enable us to predict land use changes in the study area from 2015 to 2050. Next, the
 151 statistical maize yield model was incorporated to predict maize yield per hectare under the
 152 impact of temperature, precipitation, agricultural technology and sunshine hours in four
 153 Representative Concentration Pathways (RCPs). Then, total maize yields under different
 154 scenarios were assessed based on the product of the simulated maize planting area and the
 155 predicted maize yield per hectare, and compared at two time periods of 2011-2030 and 2031-
 156 2050.



157

158 **Figure 2.** The analytical framework of future maize yield.

159 3.2 Future climate scenario design

160 Future scenarios are designed based on four RCP descriptions in CMIP5, a standard
 161 experiment protocol to define a series of coupled atmosphere-ocean general circulation models
 162 developed by Climate Modeling Groups, World Climate Research Project (WCRP), and
 163 International Geosphere-Biosphere Project (IGBP) ([Kriegler et al., 2014](#); [O'Neill et al., 2014](#);
 164 [Pan et al., 2020](#); [van Vuuren and Carter, 2014](#)). The four RCPs reflect the radiative forcing levels
 165 of 2.6, 4.5, 6.0 and 8.5 W/m² by 2100. Each RCP pathway describes a range of climatic and
 166 socio-economic characteristics related to different levels of carbon emissions ([van Vuuren and](#)
 167 [Carter, 2014](#)), i.e., average temperature and precipitation in the growing season (**Figure S1**), and
 168 agricultural mechanization promotion ([Rotz et al., 2019](#)). Average temperature and precipitation
 169 under four RCPs were set according to historical and projected climate datasets. The growth
 170 rates of agricultural technology under four RCPs were determined to simulate the future maize
 171 yield based on the actual development of Jilin Province and previous research experience (**Table**
 172 **2**).

173 **Table 2**174 *The growth rate of agriculture technology*

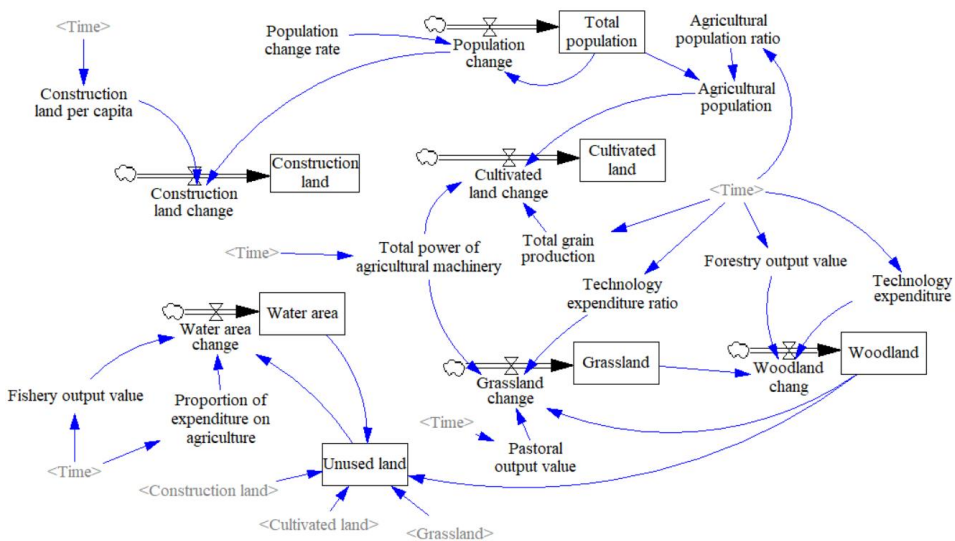
Scenarios		Growth rate
RCP 2.6	Level	High
	Growth rate	+7%
RCP 4.5	Level	Relatively high
	Growth rate	+5%
RCP 6.0	Level	Moderate
	Growth rate	+3%
RCP 8.5	Level	Low
	Growth rate	0

175

176 3.3 Projection of future land use demand

The prediction of the planting area of maize consists of two steps: land use demand projection and spatial pattern allocation. In the first step, future land use demands were projected using the system dynamic (SD) model. The SD model enables us to simulate the complex evolution process of the land system through the feedback and interaction between different elements ([Akhtar et al., 2013](#)).

The SD model in this study comprises three sections: population, social economy, and land use (**Figure 3**). The population section represents urban and rural changes related to socio-economic development and land use demands for urban and rural settlements and agricultural production. The socio-economic section considers the effect of agricultural technology development and fixed asset investment change on agriculture, forestry, and fishing production. Further, the land use section illustrates land use conversions and their driving forces in terms of population, socio-economic development and interaction among various land use types ([Liu et al., 2017](#)). For example, cultivated land may expand due to a series of farmland supplementation measures, e.g., the consolidation of rural settlements and the reclamation of wild grassland, and will decline because of farmland reforestation and urban encroachment. The interaction and feedback among the three sections are defined through regression methods. The time range of the SD model in this study is from 2011 to 2050, and the time step is one year. Outputs of the SD were used to limit land use quantities in the spatial land use pattern allocation.



195

Figure 3. Interaction and feedback relationships in the system dynamic model.

197 3.4 Allocation of spatial land use pattern

198 The spatial pattern of land use was allocated using the FLUS model based on the land use
 199 demand from the SD. The FLUS consists of two modules ([Liu et al., 2017](#)): (1) estimating the
 200 occurrence probability of each land use type on a specific grid unit based on a three-layer
 201 artificial neural network (ANN); (2) determining the land use type of each grid cell based on the
 202 cellular automata (CA) approach. Specifically, the three-layer ANN was trained using the
 203 empirical land use data and various driving factors that combine socio-economic and natural
 204 effects, including population density, GDP, elevation, slope, aspect, distance to main highways,
 205 distance to primary railways, distance to rivers, and distance to cities ([Yang et al., 2020](#)). The
 206 CA calculates the combined probability of a specific land use type on each grid cell based on the
 207 product of the occurrence probability, land use conversion cost, spatial neighborhood effect and
 208 land use inertia coefficient ([Li et al., 2017](#)), and then allocates the suitable land use type to each
 209 grid cell using the roulette selection method ([Pan et al., 2020](#)). See [Yang et al. \(2020\)](#) for detailed
 210 model descriptions and parameterizations.

211 3.5 Estimation of maize yield per hectare

212 Maize yield per hectare was estimated using a regression analysis based on the historical
 213 data of maize production from 2000 to 2015. A series of essential factors for photosynthesis and
 214 plant growth in terms of county-level differences, socio-economic development and physical
 215 conditions were selected as independent variables, including the mean and variance of
 216 temperature and precipitation in the growing season([Lobell et al., 2011; Urban et al., 2012](#)), the
 217 total power of agricultural machinery, and sunshine hours ([Murkie and Niyogi, 2011](#)).
 218 Considering the non-linear relationship between climate variables and maize yields and
 219 moderately/strongly skewed distribution of maize yields ([Huang et al., 2021](#)), the logarithm of
 220 the maize yield rather than the yield *per se* was used as the dependent variable. Moreover, the
 221 quadratic function has been proved promising in simulating the dynamic relationship between
 222 climate conditions and maize yield ([Grassini et al., 2009; Lobell and Burke, 2010](#)).

223 The regression model for the estimation of per unit maize yield can be expressed as
 224 follows:

$$225 \quad \log(\hat{y}) = \beta_0 + \beta_1 machine + \beta_2 machine^2 + \beta_3 T + \beta_4 T^2 + \beta_5 P + \beta_6 P^2 + \beta_7 SH + \\ 226 \quad \sum \beta_i county_i \quad (1)$$

227 where T , P , and SH represent the temperature, precipitation, and sunshine hours during
 228 the growing season from May to September. *county* is a dummy variable to capture the spatially
 229 heterogeneous influence of physical and socio-economic factors at the county level, such as soil
 230 quality and agronomic. *machine* accounts for an improvement in agricultural mechanization.
 231 Square terms of independent variables denote a certain degree of nonlinearity (see **Text S1** and
 232 **Table S1** for detailed parameters).

233 Moreover, the average change of maize yield often accompanies its variance change. The
 234 variance of per hectare yield can measure the stability of the inter-annual production of maize,
 235 which is significant in maintaining the steady income of farmers and ensuring regional food
 236 security. The yield variance can be calculated in the following:

$$237 \quad Var(y) = (E[\log(\hat{y})])^2 \times Var(\log(\epsilon)) + (E[\log(\epsilon)])^2 \times Var(\log(\hat{y})) + \\ 238 \quad Var(\log(\hat{y})) \times Var(\log(\epsilon)) \quad (2)$$

239 where $Var(y)$ refers to the variance of yield per hectare in each county, and ϵ refers to
 240 the residual yield per hectare.

241 We used the residuals of training data (**Table S2**) to calculate the expected $Var(y)$.
 242 Therefore, we assumed that the yield residual would not change with the change of predicted
 243 climate. To verify this hypothesis, we conducted least square regression between the yield
 244 residuals' square $[\log(\epsilon)]^2$ and the average T and P in the training period. The results showed
 245 that climate change causes a slight change in $[\log(\epsilon)]^2$ (**Figure S2**). Therefore, in this study, the
 246 assessment results of yield variation under future climate will be relatively conservative.

247 3.6 Model implementation and evaluation

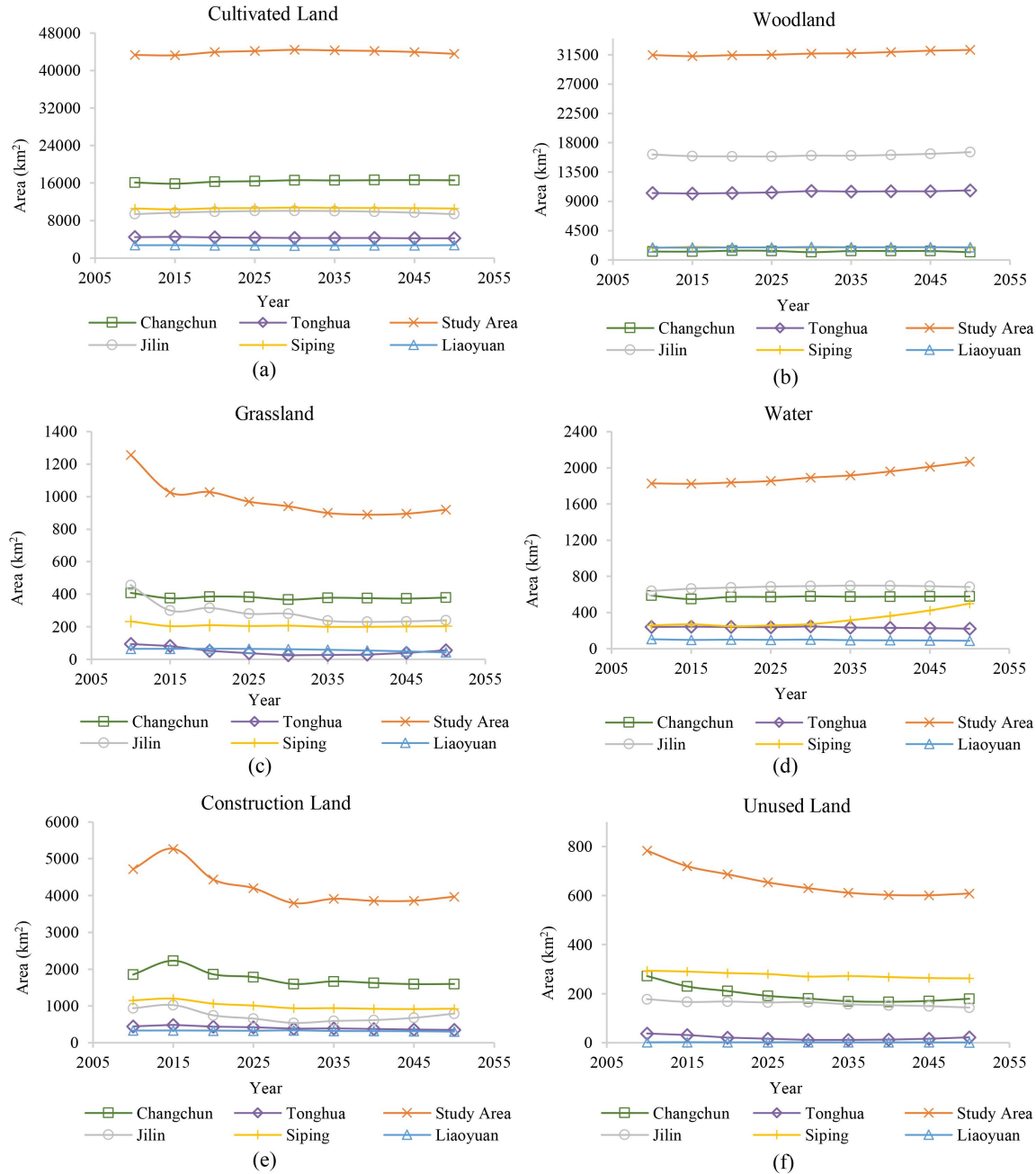
248 The SD model was built with Vensim (<https://vensim>), and the FLUS was performed in
 249 the GEOSOS platform. The empirical land use data in 2000 and 2015 were used to train and
 250 validate the simulation model. Kappa coefficient was used to evaluate the accuracy of land use
 251 simulation. Overall, the average accuracy rate exceeds 80%, and the Kappa coefficient reaches
 252 0.65, indicating the positive performance of the FLUS. Further, regression analysis was
 253 conducted in SPSS. The standardized residuals of the regression model obey the normal
 254 distribution, and R^2 equals 0.436. These experimental results indicate the good performance of
 255 the proposed framework for maize yield projections.

256 **4 Results and analysis**

257 4.1 Dynamic land use changes

258 The study area will experience slight changes in cultivated land and woodland, and
259 remarkable changes in construction land, grassland, water areas and unused land by 2050. Land
260 use changes will exhibit evident spatial differences across the study area (**Figure 4** and **Figure**
261 **S3**). As for cultivated land, the total area will slightly increase from 43,321.70 km² in 2010 to
262 43,556.00 km² in 2050, with an inverted U-shaped trend. Specifically, the cultivated land will
263 increase to 44,424.08 km² in 2030 and then drop by 867.61 km² from 2030 to 2050. However,
264 the trend will differ at the city level. The cultivated land in Changchun and Liaoyuan will
265 increase by 485.68 km² and 19.62 km² in 2010-2050, while those in Tonghua, Jilin and Siping
266 will decrease by 252.12 km², 11.33 km², and 3.88 km².

267



268

269

Figure 4. The changes in land use quantities from 2010 to 2050.

270

The gain and loss of cultivated land will be $3,796.69 \text{ km}^2$ and $3,561.53 \text{ km}^2$, respectively

271

(Figure 5f). Specifically, 43.09% and 40.03% of farmland gain will be attributed to the reduction of woodland and construction land, for example, the consolidation of scattered rural settlements originating from rural population shrinkage (Liu et al., 2013b). In turn, 63.71% of farmland loss will be attributed to farmland reforestation, which indicates the Chinese government's emphasis

272

273

274

on ecological protection ([Shan et al., 2020](#)). At the city level, Changchun has the highest farmland gain (**Figure 5a**). The gain of cultivated land will be 1,080.04 km², and 59.45% comes from the consolidation of construction land. As a central city in Northeast China, increasing cultivated land will alleviate the pressure of increasing population on food production ([Zhang et al., 2012](#)). Conversely, Tonghua has the largest reduction of arable land (**Figure 5e**). The gain and loss of cultivated land will be 471.00 km² and 722.52 km², respectively. It can be observed that 627.28 km² of cultivated land in this city will be converted into forest land. Liaoyuan, Siping and Jilin are likely to experience slight farmland gain or loss; these changes are less than 20 km² (**Figure 5b, c, and d**).

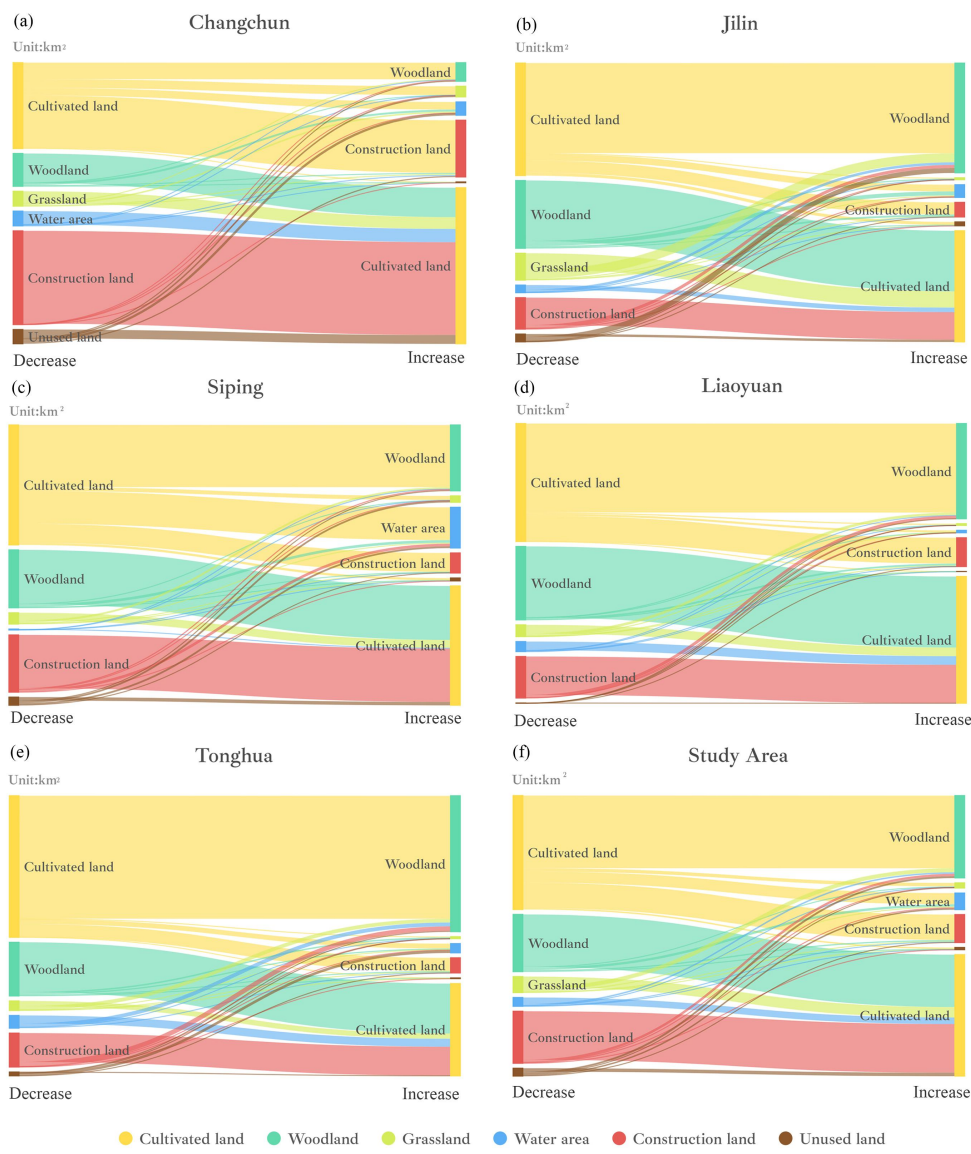
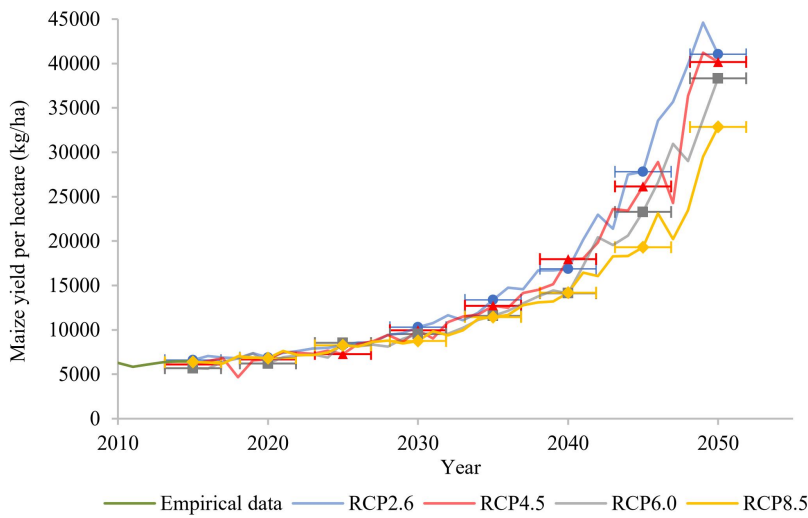


Figure 5. Land use conversions from 2010 to 2050.

286 4.2 Changes in maize yield per hectare in different scenarios

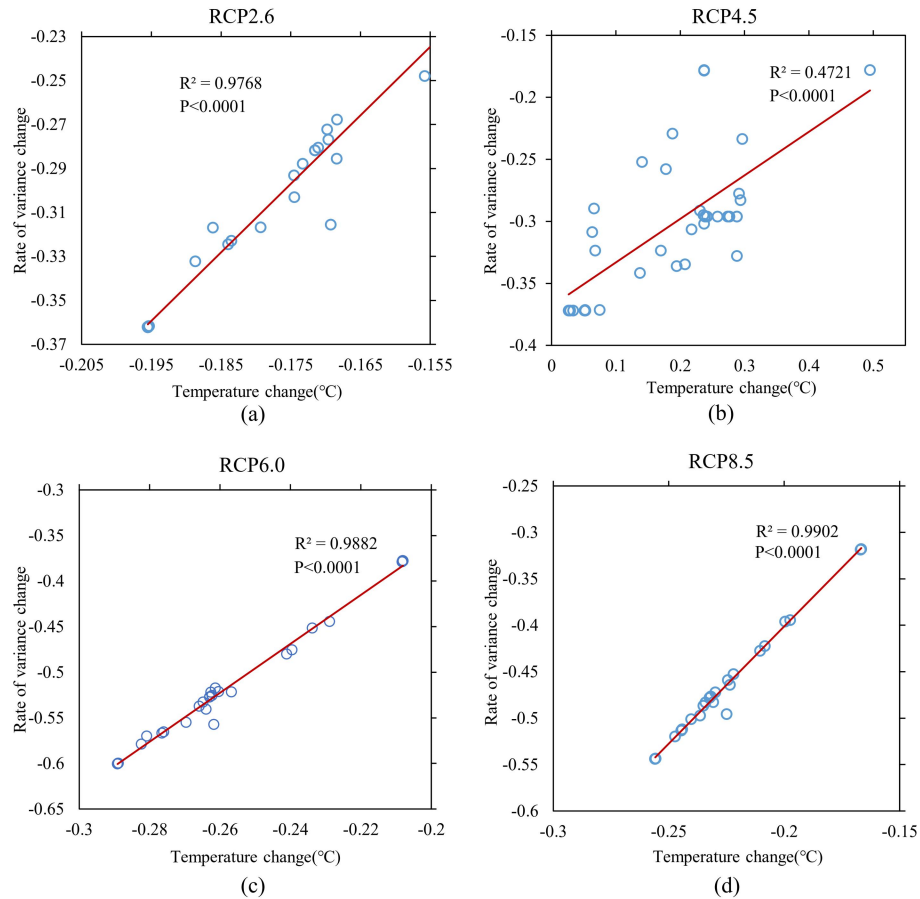
287 The maize yield per hectare is likely to exhibit a two-stage upward trend from 2011 to
 288 2050 (**Figure 6**). From 2011 to 2030, it will moderately increase by 76.32%, 70.63%, 63.278%,
 289 49.66% under RCP2.6, 4.5, 6.0, 8.5, respectively. From 2031 to 2050, however, it will
 290 experience a corresponding sharp promotion of 280.74%, 344.91%, 299.64%, and 233.352%.



291

292 **Figure 6.** Changes in average maize yield per hectare under four RCP scenarios from
 293 2011 to 2050. Standard Errors of Mean (SEM) of RCP 2.6, 4.5, 6.0, and 8.5 are 1575.51,
 294 1401.41, 1252.26, and 975.38 kg/ha, respectively.

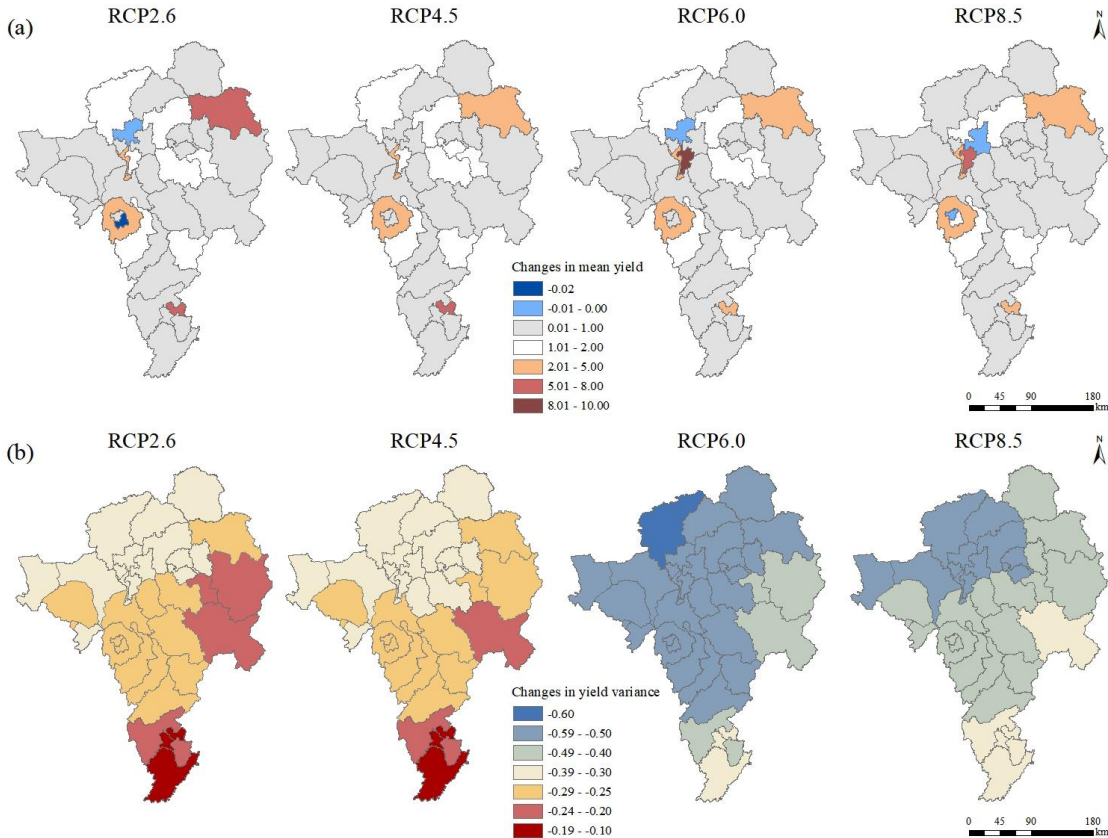
295 Climate change (**Figure S4**) may exert different effects on per unit maize yield over time.
 296 RCP 2.6 will have the maximum annual growth rate of the per-unit yield up to 34.73%, with a
 297 mean value of 14175.00 kg/ha. Conversely, RCP 8.5 is likely to exhibit the minimum increase of
 298 the per-unit yield by 11324.47 kg/ha with an annual growth rate of 33.78%. A positive
 299 correlation between the per-unit yield promotion and the radiative forcing levels caused by
 300 greenhouse gas emissions can be observed, and a growing gap in the per unit yields under four
 301 RCP scenarios will also arise over time. We further found that temperature strongly correlates
 302 with the changing rate of the maize yield variance (**Figure 7**). In RCP2.6, RCP6.0, RCP8.5, R^2
 303 can reach up to 0.99 ($p < 0.0001$), while that in RCP4.5 is only 47.21%. The temperature changes
 304 primarily lead to yield variance.



305

306 **Figure 7.** Correlation analysis between temperature and variance transformation rate
307 under four RCP scenarios.

308 At the county level, the yield variations under the four RCPs range from 0.72 to 32.82
309 from 2011 to 2030, varying from 0.82 to 32.87 in 2031-2050. In contrast, the mean per unit yield
310 gap in the four RCPs will be much greater from 2031 to 2050. For example, the range of RCP2.6
311 in 2031-2050 can expand to 10 times that in 2011-2030. Despite the different distribution of
312 values, the mean yields still exhibit a positive correlation with the variances. The spatial
313 distribution of relative change in the mean yield per hectare and its variance in these two periods
314 are similar, with a significant increase in the northern and central regions and a slight increase or
315 decrease in the western region. Most counties had a similar change rate of average yield under
316 the four RCPs, but the gaps under RCP2.6 and RCP6.5 are much larger (**Figure 8a**). From the
317 perspective of the distribution area, RCP6.5 and RCP8.5 have a greater relative reduction of
318 variance from 2011-2030 to 2031-2050 (**Figure 8b**).



319

320 **Figure 8.** Rate of changes in means (a) and variances (b) of the per unit maize yield
 321 during the periods of 2011-2030 and 2031-2050.

322 4.3 Changes in total maize yield

323 The total maize yield will significantly increase from 2011 to 2050, with a growth rate of
 324 78.71% (RCP2.6), 79.40% (RCP4.5), 79.01% (RCP6.0) and 78.63% (RCP8.5). In the first two
 325 decades, the total yield under RCP2.6, RCP4.5, RCP6.0, and RCP8.5 moderately increase by
 326 38.61%, 35.61%, 30.03% and 18.28%, then exhibit sharp promotion to 124.92%, 149.01%,
 327 148.19% and 161.00% in the latter twenty years. The total maize yields under four RCP
 328 scenarios will remarkably differ. Specifically, RCP 2.6 has the maximum total yield of 24.02
 329 megatons in 2030, but it will rank third in 2050. RCP4.5 ranks second in 2030 with 23.50
 330 megatons of maize yield, while it will reach the highest value of 58.52 megatons in 2050.
 331 Notably, the total maize yield under RCP 8.5 will remain the minimum in 2030 and 2050 (**Table**
 332 **3**).

333

334

Table 3

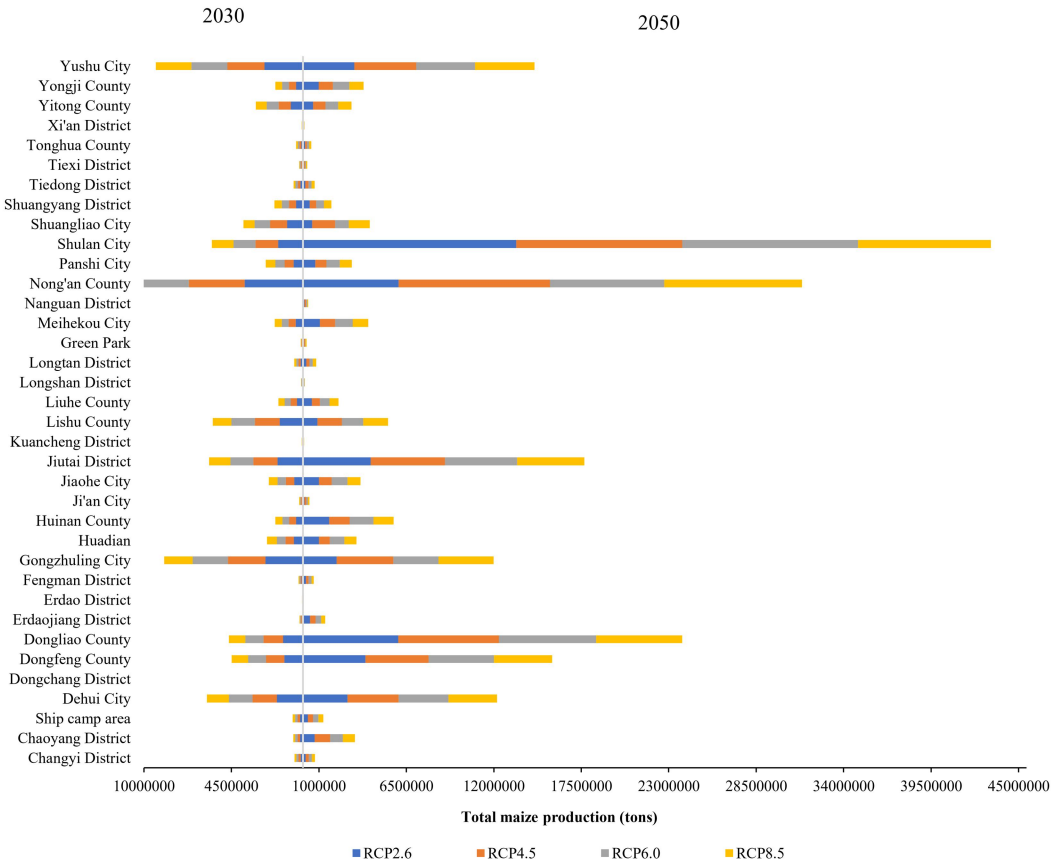
335

Total maize yields in 2030 and 2050 under four RCP scenarios

Scenarios	2030(megatons)	change rate 2011-2030	2050(megatons)	change rate 2030-2050
RCP2.6	24.02	38.61%	54.03	124.92%
RCP4.5	23.50	35.61%	58.52	149.01%
RCP6.0	22.54	30.03%	55.93	148.19%
RCP8.5	20.50	18.28%	53.50	161.00%

336

337 Changes in total maize yields will be simultaneously influenced by the per-unit yield and
 338 the planting area. In urban areas, e.g., Changchun, Jilin, and Chaoyang, Nanguan and Erdao
 339 District of Liaoyuan only have low total yields of maize even if the per-unit yield is at the middle
 340 or upper level. In contrast, some counties, such as Nong'an and Gongzhuling, with low per-unit
 341 yields will feature higher maize production due to their larger maize planting areas (**Figure 9**).
 342 From 2030 to 2050, 67% of counties will experience a decline in cultivated land (**Figure S5**), but
 343 the total maize yields of these counties will increase due to the promotion of per hectare maize
 344 yield. Furthermore, climate change will alter the orders of some counties with large planting
 345 areas of maize in terms of total yields, e.g., Liuhe, Lishu, Fengman, Dongliao, and Dongfeng
 346 County. Under PCR2.6, a slowdown of growth rate in maize yield per hectare in these counties
 347 leads to the decline of the total yield ranking. Conversely, RCP8.5 will ensure that most counties
 348 have a high total production ranking due to its relatively high growth rate of per-unit yield.



349

350

Figure 9. Total maize production at the county level under four scenarios.351 **5 Discussion**352 **5.1 Comprehensive impact on maize yield**

353 Unlike the previous study, our framework examines the synergistic effects of climate
 354 change and land use change on the yield of rain-fed maize in a phaeozem region of Jilin Province.
 355 The results show that there appears to be a clear contrast in total yield, potential increment, and
 356 spatial pattern between different scenarios, and balanced development is more conducive to
 357 maintaining a steady increase in total maize production. For example, Potential maize yield per
 358 hectare will significantly increase under the four climate change scenarios from 2011 to 2050,
 359 ranked as: RCP2.6>RCP4.5>RCP6.0>RCP8.5. However, RCP2.6 and RCP6.0 will have
 360 differences in the maize yield among counties, while RCP4.5 will exhibit a balanced regional
 361 pattern of maize production (**Figure 8a**). The total maize yield in 2050 will peak under the
 362 RCP4.5 scenario, suggesting the combined effect of temperature, precipitation, and technological

363 progress on maize growth is the best. This scenario's moderate carbon emissions and population
 364 and economic growth will help coordinate the conflicts between farmland protection and
 365 vegetation conservation and increase overall maize production simultaneously ([Hou and Li, 2021](#); [Zhang and Qi, 2010](#)). Notably, an increase in per hectare yield could mitigate the impact
 366 of farmland loss on maize yields. The total yield of RCP2.6, RCP4.5, RCP6.0, and RCP8.5 will
 367 reach 54.03, 58.52, 55.93, and 53.50 megatons by 124.92%, 149.01%, 148.19% and 161.00%
 368 from 2030 to 2050. Although a large amount of cultivated land will be occupied by forest and
 369 grassland, the total maize yield under all scenarios still increased exponentially.
 370

371 The variance of temperature and precipitation during the growing season will affect yield
 372 variance ([Urban et al., 2012](#)). With the increase in precipitation variance, the variance of maize
 373 yields during the period of 2031-3050 will get higher than that in 2011-2030. Under the threat of
 374 maize yield reduction caused by variable or extreme climates ([Feng et al., 2021](#); [Malik et al., 2021](#)), how to formulate adaptation and mitigation strategies will be a challenging long-term
 375 issue for land managers ([Iglesias and Garrote, 2015](#); [Zobeidi et al., 2021](#)).
 376

377 5.2 Policy implications

378 Our study suggested several implications for agricultural land use and maize production.
 379 We can solve many uncertain problems in agricultural production by considering the present and
 380 predicted near future land-use, economic and climate scenarios. For example, agricultural
 381 technology development can balance land use change, climate change and maize production due
 382 to its positive impact on per unit yield ([Rojas-Downing et al., 2017](#)). Previous studies suggested
 383 that diversification of maize varieties can improve maize resistance to external disturbances
 384 caused by extreme weather events and human activities ([Lin et al., 2008](#)) ([Altieri and Nicholls, 2017](#)). Maize breeding and biotechnology also have the enormous biological potential to increase
 385 grain yield ([Foulkes et al., 2011](#)). Researchers have proven that organic matter enhances
 386 underground biodiversity, thereby creating suitable conditions for plant roots ([Diaz-Zorita et al., 1999](#)). Moreover, regular training and technical guidance for farmers can improve their risk
 388 awareness and ability to deal with the risk ([Olesen et al., 2011](#)). We suggest that the investment
 389 in maize variety and planting technology development should be encouraged to promote the per
 390 unit yield of maize. Indeed, accurate prediction of climate change and rational planning of
 391

392 planting scale and planting pattern can advance the reasonability of agricultural management
 393 strategies.

394 5.3 Advantages and limitations

395 By combining the FLUS and the statistical yield model, this research framework can
 396 better describe the joint impact of climate change and land use change on maize yield.
 397 Meanwhile, the framework is flexible and can be used as a general decision-making tool for land
 398 planning and maize management in different situations. This study documented that climate
 399 change will positively impact maize yields in the study area, which is consistent with other
 400 simulation studies ([Liang et al., 2019](#); [Pu et al., 2020](#); [Zhang et al., 2017a](#)). Since the study area
 401 locates in the cold temperate zone, global warming could reduce cold damage and extend the
 402 growing season, which will benefit maize yields ([Zongruing et al., 2007](#)). From an optimistic
 403 point of view, we expect further improvement in planting efficiency (maize yield) as agricultural
 404 technology advances and planting management improves in the future. Moreover, the effect of
 405 human irrigation on maize growth has been excluded by selecting the study area in a rain-fed
 406 region.

407 This work still has several limitations. First, uncertainty in future climate change will
 408 impact the simulation accuracy. The climate conditions shown by different general circulation
 409 models (GCMs) in the same region may be quite different ([Liu et al., 2013a](#); [Tatsumi et al.,
 410 2011](#)). The BCC_CSM1.1 m model was selected for this study to better eliminate the possible
 411 errors in the prediction results. Although the BCC has been applied to a number of studies on
 412 grain production in northeast China ([Pu et al., 2020](#); [Xie et al., 2020](#)), there is still room for
 413 improvement. Second, existing studies have shown that incorporating remote sensing into
 414 statistical models can improve forecasting accuracy, especially for large-scale regions ([Laudien
 415 et al., 2020](#)).

416 **6 Conclusion**

417 This study proposes an integrated framework for maize yield prediction by combining the
 418 SD and the FLUS model with the statistical model. Future maize yield change can be simulated
 419 under the four RCP scenarios. The proposed framework is flexible and suitable for applications

420 in any other regional studies. The simulations help provide scientific guidance for the decision-
421 making of agricultural management.

422 We conclude that an increase in per-unit yield in the study area will mitigate the negative
423 impact of farmland loss on the total maize yield. Although cultivated land is likely to decrease
424 from 2030 to 2050, the total maize yields under RCP2.6, 4.5, 6.0, and 8.5 will still increase by
425 124.92%, 149.01%, 148.19% and 161.00%. Under the four RCPs, disparities in total maize
426 yields will differ across the region, especially under RCP2.6. In comparison, RCP 4.5 features
427 more balanced and stable, which will be conducive to ensuring maize yields and benefitting
428 regional sustainable development in the future.

429 Facing the threat of variable or extreme climates and the further widened yield gap
430 between different counties, we need to implement the differentiated policies of agricultural
431 production and farmland protection, including strengthening cultivated land protection and crop
432 management in low-yield areas, as well as adoption of adaptation and mitigation measures.

433

434 **Acknowledgments**

435 This research was funded by the National Natural Science Foundation of China [Grant
436 number: 41771429; 42171414].

437

438 **Data Availability Statement**

439 In this study, GCMs data are downloaded on the WDCC platform through
440 [https://doi.org/10.1594/WDCC/ETHr2\(Knutti, 2014\)](https://doi.org/10.1594/WDCC/ETHr2(Knutti, 2014)). Historical climate data are available at the
441 National Meteorological Sciences Data Center (<http://data.cma.cn/>) by searching the "China
442 Terrestrial Climate Standard Monthly Values Dataset". The grid dataset of China's GDP and
443 population spatial distribution are derived from the resource and environmental science data
444 registration and publication system([Xinliang, 2017a, b](#)), and can be obtained through
445 <http://www.resdc.cn/DOI>. Empirical land use maps were derived from the Chinese Academy of
446 Sciences (CAS; <http://www.resdc.cn>) ([Ning et al., 2018](#)).

447

448 **References**

- 449 Abate, M.C., Kuang, Y.-p. (2021). "The impact of the supply of farmland, level of agricultural mechanisation, and
 450 supply of rural labour on grain yields in China." *Studies in Agricultural Economics* 123, 33-42.
 451 <https://doi.org/10.7896/j.2081>
- 452 Akhtar, M.K., Wibe, J., Simonovic, S.P., MacGee, J. (2013). "Integrated assessment model of society-biosphere-
 453 climate-economy-energy system." *Environmental Modelling & Software* 49, 1-21.
 454 <https://doi.org/10.1016/j.envsoft.2013.07.006>
- 455 Akpoti, K., Kabo-bah, A.T., Zwart, S.J. (2019). "Agricultural land suitability analysis: State-of-the-art and outlooks
 456 for integration of climate change analysis." *Agricultural Systems* 173, 172-208.
 457 <https://doi.org/10.1016/j.agrsy.2019.02.013>
- 458 Altieri, M.A., Nicholls, C.I. (2017). "The adaptation and mitigation potential of traditional agriculture in a changing
 459 climate." *Climatic Change* 140, 33-45. <https://doi.org/10.1007/s10584-013-0909-y>
- 460 Asseng, S., Ewert, F., Rosenzweig, C., Jones, J.W., Hatfield, J.L., Ruane, A.C., Boote, K.J., Thorburn, P.J., Rotter,
 461 R.P., Cammarano, D., Brisson, N., Basso, B., Martre, P., Aggarwal, P.K., Angulo, C., Bertuzzi, P., Biernath, C.,
 462 Challinor, A.J., Doltra, J., Gayler, S., Goldberg, R., Grant, R., Heng, L., Hooker, J., Hunt, L.A., Ingwersen, J.,
 463 Izaurralde, R.C., Kersebaum, K.C., Mueller, C., Kumar, S.N., Nendel, C., O'Leary, G., Olesen, J.E., Osborne, T.M.,
 464 Palosuo, T., Priesack, E., Riponche, D., Semenov, M.A., Shcherbak, I., Steduto, P., Stoeckle, C., Strattonovitch, P.,
 465 Streck, T., Supit, I., Tao, F., Travasso, M., Waha, K., Wallach, D., White, J.W., Williams, J.R., Wolf, J. (2013).
 466 "Uncertainty in simulating wheat yields under climate change." *Nature Climate Change* 3, 827-832.
 467 <https://doi.org/10.1038/nclimate1916>
- 468 Banakara, K.B., Pandya, H.R., Garde, Y.A. (2019). "Pre-harvest forecast of kharif rice yield using PCA and MLR
 469 technique in Naysari district of Gujarat." *Journal of Agrometeorology* 21, 336-343.
- 470 Basse, R.M., Omrani, H., Charif, O., Gerber, P., Bodis, K. (2014). "Land use changes modelling using advanced
 471 methods: Cellular automata and artificial neural networks. The spatial and explicit representation of land cover
 472 dynamics at the cross-border region scale." *Applied Geography* 53, 160-171.
 473 <https://doi.org/10.1016/j.apgeog.2014.06.016>
- 474 Basso, B., Liu, L. (2019). "Seasonal crop yield forecast: Methods, applications, and accuracies." in: Sparks, D.L.
 475 (Ed.), *Advances in Agronomy*, Vol 154, pp. 201-255. <https://doi.org/10.1016/bs.agron.2018.11.002>
- 476 Basso, B., Liu, L., Ritchie, J.T. (2016). "A Comprehensive Review of the CERES-Wheat, -Maize and -Rice Models'
 477 Performances." in: Sparks, D.L. (Ed.), *Advances in Agronomy*, Vol 136, pp. 27-132.
 478 <https://doi.org/10.1016/bs.agron.2015.11.004>
- 479 Camberlin, P., Diop, M. (1999). "Inter-relationships between groundnut yield in Senegal, interannual rainfall
 480 variability and sea-surface temperatures." *Theoretical and Applied Climatology* 63, 163-181.
 481 <https://doi.org/10.1007/s007040050101>
- 482 Diaz-Zorita, M., Buschiazzo, D.E., Peinemann, N. (1999). "Soil organic matter and wheat productivity in the
 483 semiarid argentine pampas." *Agronomy Journal* 91, 276-279.
 484 <https://doi.org/10.2134/agronj1999.00021962009100020016x>
- 485 Feng, S., Hao, Z., Zhang, X., Hao, F. (2021). "Changes in climate-crop yield relationships affect risks of crop yield
 486 reduction." *Agricultural and Forest Meteorology* 304. <https://doi.org/10.1016/j.agrformet.2021.108401>
- 487 Foulkes, M.J., Slafer, G.A., Davies, W.J., Berry, P.M., Sylvester-Bradley, R., Martre, P., Calderini, D.F., Griffiths,
 488 S., Reynolds, M.P. (2011). "Raising yield potential of wheat. III. Optimizing partitioning to grain while maintaining
 489 lodging resistance." *Journal of Experimental Botany* 62, 469-486. <https://doi.org/10.1093/jxb/erq300>
- 490 Gao, J., Yang, X., Zheng, B., Liu, Z., Zhao, J., Sun, S. (2020). "Does precipitation keep pace with temperature in the
 491 marginal double-cropping area of northern China?" *European Journal of Agronomy* 120.
 492 <https://doi.org/10.1016/j.eja.2020.126126>
- 493 Giri, A.K., Bhan, M., Agrawal, K.K. (2017). "Districtwise wheat and rice yield predictions using meteorological
 494 variables in eastern Madhya Pradesh." *Journal of Agrometeorology* 19, 366-368.
- 495 Grassini, P., Yang, H., Cassman, K.G. (2009). "Limits to maize productivity in Western Corn-Belt: A simulation
 496 analysis for fully irrigated and rainfed conditions." *Agricultural and Forest Meteorology* 149, 1254-1265.
 497 <https://doi.org/10.1016/j.agrformet.2009.02.012>
- 498 He, Y., Liang, H., Hu, K., Wang, H., Hou, L. (2018). "Modeling nitrogen leaching in a spring maize system under
 499 changing climate and genotype scenarios in arid Inner Mongolia, China." *Agricultural Water Management* 210, 316-
 500 323. <https://doi.org/10.1016/j.agwat.2018.08.017>
- 501 Hengl, T., de Jesus, J.M., Heuvelink, G.B.M., Gonzalez, M.R., Kilibarda, M., Blagotic, A., Shangguan, W., Wright,
 502 M.N., Geng, X., Bauer-Marschallinger, B., Guevara, M.A., Vargas, R., MacMillan, R.A., Batjes, N.H., Leenaars,

- 503 J.G.B., Ribeiro, E., Wheeler, I., Mantel, S., Kempen, B. (2017). "SoilGrids250m: Global gridded soil information
 504 based on machine learning." *Plos One* 12. <https://doi.org/10.1371/journal.pone.0169748>
- 505 Hou, R., Li, H. (2021). "Spatial-Temporal Change and Coupling Coordination Characteristics of Land Use
 506 Functions in Wuhan City: Based on the Comparison Before and After the Resource-economical and Environment-
 507 friendly Society Experimental Zone Establishment." *China Land Science* 35, 69-78.
- 508 Huang, J.Y., Hartemink, A.E., Kucharik, C.J. (2021). "Soil-dependent responses of US crop yields to climate
 509 variability and depth to groundwater." *Agricultural Systems* 190. <https://doi.org/10.1016/j.agsy.2021.103085>
- 510 Iglesias, A., Garrote, L. (2015). "Adaptation strategies for agricultural water management under climate change in
 511 Europe." *Agricultural Water Management* 155, 113-124. <https://doi.org/10.1016/j.agwat.2015.03.014>
- 512 Jiang, R., He, W., He, L., Yang, J.Y., Qian, B., Zhou, W., He, P. (2021). "Modelling adaptation strategies to reduce
 513 adverse impacts of climate change on maize cropping system in Northeast China." *Scientific Reports* 11.
<https://doi.org/10.1038/s41598-020-79988-3>
- 514 Kang, Y., Ozdogan, M., Zhu, X., Ye, Z., Hain, C., Anderson, M. (2020). "Comparative assessment of environmental
 515 variables and machine learning algorithms for maize yield prediction in the US Midwest." *Environmental Research
 516 Letters* 15. <https://doi.org/10.1088/1748-9326/ab7df9>
- 517 Knutti, R. (2014). "IPCC Working Group I AR5 snapshot: The rcp26 experiment." [Dataset].
<https://doi.org/10.1594/WDCC/ETHr2>
- 518 Kolotii, A., Kussul, N., Shelestov, A., Skakun, S., Yailymov, B., Basarab, R., Lavreniuk, M., Oliynyk, T., Ostapenko,
 519 V. (2015). "COMPARISON OF BIOPHYSICAL AND SATELLITE PREDICTORS FOR WHEAT YIELD
 520 FORECASTING IN UKRAINE." in: Schreier, G., Skrovseth, P.E., Staudenrausch, H. (Eds.), 36th International
 521 Symposium on Remote Sensing of Environment, pp. 39-44. <https://doi.org/10.5194/isprsarchives-XL-7-W3-39-2015>
- 522 Kowalik, W., Dabrowska-Zielinska, K., Meroni, M., Racza, T.U., de Wit, A. (2014). "Yield estimation using
 523 SPOT-VEGETATION products: A case study of wheat in European countries." *International Journal of Applied
 524 Earth Observation and Geoinformation* 32, 228-239. <https://doi.org/10.1016/j.jag.2014.03.011>
- 525 Kriegler, E., Edmonds, J., Hallegatte, S., Ebi, K.L., Kram, T., Riahi, K., Winkler, H., van Vuuren, D.P. (2014). "A
 526 new scenario framework for climate change research: the concept of shared climate policy assumptions." *Climatic
 527 Change* 122, 401-414. <https://doi.org/10.1007/s10584-013-0971-5>
- 528 Laudien, R., Schuberger, B., Makowski, D., Gornott, C. (2020). "Robustly forecasting maize yields in Tanzania
 529 based on climatic predictors." *Scientific Reports* 10. <https://doi.org/10.1038/s41598-020-76315-8>
- 530 Leng, G., Hall, J.W. (2020). "Predicting spatial and temporal variability in crop yields: an inter-comparison of
 531 machine learning, regression and process-based models." *Environmental Research Letters* 15.
<https://doi.org/10.1088/1748-9326/ab7b24>
- 532 Li, X., Chen, G.Z., Liu, X.P., Liang, X., Wang, S.J., Chen, Y.M., Pei, F.S., Xu, X.C. (2017). "A New Global Land-
 533 Use and Land-Cover Change Product at a 1-km Resolution for 2010 to 2100 Based on Human-Environment
 534 Interactions." *Annals of the American Association of Geographers* 107, 1040-1059.
<https://doi.org/10.1080/24694452.2017.1303357>
- 535 Li, Y., Hu, Z., Wang, X., Wu, M., Zhou, H., Zhang, Y. (2020). "Characterization of a polysaccharide with
 536 antioxidant and anti-cervical cancer potentials from the corn silk cultivated in Jilin province." *International Journal
 537 of Biological Macromolecules* 155, 1105-1113. <https://doi.org/10.1016/j.ijbiomac.2019.11.077>
- 538 Liang, S., Zhang, X.B., Sun, N., Li, Y.F., Xu, M.G., Wu, L.H. (2019). "Modeling crop yield and nitrogen use
 539 efficiency in wheat and maize production systems under future climate change." *Nutrient Cycling in Agroecosystems*
<https://doi.org/10.1007/s10705-019-10013-4>
- 540 Lin, B.B., Perfecto, I., Vandermeer, J. (2008). "Synergies between Agricultural Intensification and Climate Change
 541 Could Create Surprising Vulnerabilities for Crops." *Bioscience* 58, 847-854. <https://doi.org/10.1641/b580911>
- 542 Liu, J., Folberth, C., Yang, H., Rockstrom, J., Abbaspour, K., Zehnder, A.J.B. (2013a). "A Global and Spatially
 543 Explicit Assessment of Climate Change Impacts on Crop Production and Consumptive Water Use." *Plos One* 8.
<https://doi.org/10.1371/journal.pone.0057750>
- 544 Liu, M., Zhang, X., Ma, Y., Xu, H. (2013b). "Evaluation of rural residential land consolidation potential using
 545 entropy weight extension model -A case study of Taihang Mountain piedmont plain in Hebei Province." *Chinese
 546 Journal of Eco-Agriculture* 21, 1166-1172.
- 547 Liu, X.P., Liang, X., Li, X., Xu, X.C., Ou, J.P., Chen, Y.M., Li, S.Y., Wang, S.J., Pei, F.S. (2017). "A future land
 548 use simulation model (FLUS) for simulating multiple land use scenarios by coupling human and natural effects."
 549 *Landscape and Urban Planning* 168, 94-116. <https://doi.org/10.1016/j.landurbplan.2017.09.019>

- 557 Liu, Y., Ren, H.-L., Klingaman, N.P., Liu, J., Zhang, P. (2021). "Improving long-lead seasonal forecasts of
 558 precipitation over Southern China based on statistical downscaling using BCC_CSM1.1m." *Dynamics of
 559 Atmospheres and Oceans* 94. <https://doi.org/10.1016/j.dynatmoce.2021.101222>
- 560 Liu, Z.-j., Yang, X.-g., Wang, W.-f., Li, K.-n., Zhang, X.-y. (2009). "Characteristics of agricultural climate
 561 resources in three provinces of northeast China under global climate change." *Ying yong sheng tai xue bao = The
 562 journal of applied ecology* 20, 2199-2206.
- 563 Lobell, D.B., Burke, M.B. (2010). "On the use of statistical models to predict crop yield responses to climate
 564 change." *Agricultural and Forest Meteorology* 150, 1443-1452. <https://doi.org/10.1016/j.agrformet.2010.07.008>
- 565 Lobell, D.B., Schlenker, W., Costa-Roberts, J. (2011). "Climate Trends and Global Crop Production Since 1980."
 566 *Science* 333, 616-620. <https://doi.org/10.1126/science.1204531>
- 567 Loboguerrero, A.M., Campbell, B.M., Cooper, P.J.M., Hansen, J.W., Rosenstock, T., Wollenberg, E. (2019). "Food
 568 and Earth Systems: Priorities for Climate Change Adaptation and Mitigation for Agriculture and Food Systems."
 569 *Sustainability* 11. <https://doi.org/10.3390/su11051372>
- 570 Malik, M.A., Wani, A.H., Mir, S.H., Ul Rehman, I., Tahir, I., Ahmad, P., Rashid, I. (2021). "Elucidating the role of
 571 silicon in drought stress tolerance in plants." *Plant Physiology and Biochemistry* 165, 187-195.
 572 <https://doi.org/10.1016/j.plaphy.2021.04.021>
- 573 Manatsa, D., Nyakudya, I.W., Mukwada, G., Matsikwa, H. (2011). "Maize yield forecasting for Zimbabwe farming
 574 sectors using satellite rainfall estimates." *Natural Hazards* 59, 447-463. <https://doi.org/10.1007/s11069-011-9765-0>
- 575 Murchie, E.H., Niyogi, K.K. (2011). "Manipulation of Photoprotection to Improve Plant Photosynthesis." *Plant
 576 Physiology* 155, 86-92. <https://doi.org/10.1104/pp.110.168831>
- 577 Mustafa, A., Heppenstall, A., Omrani, H., Saadi, I., Cools, M., Teller, J. (2018). "Modelling built-up expansion and
 578 densification with multinomial logistic regression, cellular automata and genetic algorithm." *Computers
 579 Environment and Urban Systems* 67, 147-156. <https://doi.org/10.1016/j.compenvurbsys.2017.09.009>
- 580 Ning, J., Liu, J., Kuang, W., Xu, X., Zhang, S., Yan, C., Li, R., Wu, S., Hu, Y., Du, G., Chi, W., Pan, T., Ning, J.
 581 (2018). "Spatiotemporal patterns and characteristics of land-use change in China during 2010-2015." *Journal of
 582 Geographical Sciences* 28, 547-562. <https://doi.org/10.1007/s11442-018-1490-0>
- 583 O'Neill, B.C., Kriegler, E., Riahi, K., Ebi, K.L., Hallegatte, S., Carter, T.R., Mathur, R., van Vuuren, D.P. (2014).
 584 "A new scenario framework for climate change research: the concept of shared socioeconomic pathways." *Climatic
 585 Change* 122, 387-400. <https://doi.org/10.1007/s10584-013-0905-2>
- 586 Olesen, J.E., Trnka, M., Kersebaum, K.C., Skjelvag, A.O., Seguin, B., Peltonen-Sainio, P., Rossi, F., Kozyra, J.,
 587 Micale, F. (2011). "Impacts and adaptation of European crop production systems to climate change." *European
 588 Journal of Agronomy* 34, 96-112. <https://doi.org/10.1016/j.eja.2010.11.003>
- 589 Pan, Z., He, J., Liu, D., Wang, J. (2020). "Predicting the joint effects of future climate and land use change on
 590 ecosystem health in the Middle Reaches of the Yangtze River Economic Belt, China." *Applied Geography* 124.
 591 <https://doi.org/10.1016/j.apgeog.2020.102293>
- 592 Peralta, N.R., Assefa, Y., Du, J., Barden, C.J., Ciampitti, I.A. (2016). "Mid-Season High-Resolution Satellite
 593 Imagery for Forecasting Site-Specific Corn Yield." *Remote Sensing* 8. <https://doi.org/10.3390/rs8100848>
- 594 Poornima, S., Pushpalatha, M. (2019). "Prediction of Rainfall Using Intensified LSTM Based Recurrent Neural
 595 Network with Weighted Linear Units." *Atmosphere* 10. <https://doi.org/10.3390/atmos10110668>
- 596 Pu, L.M., Zhang, S.W., Yang, J.H., Chang, L.P., Xiao, X.M. (2020). "Assessing the impact of climate changes on
 597 the potential yields of maize and paddy rice in Northeast China by 2050." *Theoretical and Applied Climatology* 140,
 598 167-182. <https://doi.org/10.1007/s00704-019-03081-7>
- 599 Roebeling, R.A., Van Putten, E., Genovese, G., Rosema, A. (2004). "Application of Meteosat derived
 600 meteorological information for crop yield predictions in Europe." *International Journal of Remote Sensing* 25, 5389-
 601 5401. <https://doi.org/10.1080/01431160410001705024>
- 602 Rojas-Downing, M.M., Nejadhashemi, A.P., Harrigan, T., Woznicki, S.A. (2017). "Climate change and livestock:
 603 Impacts, adaptation, and mitigation." *Climate Risk Management* 16, 145-163.
 604 <https://doi.org/10.1016/j.crm.2017.02.001>
- 605 Rojas, O. (2007). "Operational maize yield model development and validation based on remote sensing and agro-
 606 meteorological data in Kenya." *International Journal of Remote Sensing* 28, 3775-3793.
 607 <https://doi.org/10.1080/01431160601075608>
- 608 Rotz, S., Gravely, E., Mosby, I., Duncan, E., Finnis, E., Horgan, M., LeBlanc, J., Martin, R., Neufeld, H.T., Nixon,
 609 A., Pant, L., Shalla, V., Fraser, E. (2019). "Automated pastures and the digital divide: How agricultural technologies
 610 are shaping labour and rural communities." *Journal of Rural Studies* 68, 112-122.
 611 <https://doi.org/10.1016/j.jrurstud.2019.01.023>

- 612 Sakamoto, T. (2020). "Incorporating environmental variables into a MODIS-based crop yield estimation method for
 613 United States corn and soybeans through the use of a random forest regression algorithm." *Isprs Journal of
 614 Photogrammetry and Remote Sensing* 160, 208-228. <https://doi.org/10.1016/j.isprsjprs.2019.12.012>
- 615 Shan, Y., Huang, Q., Guan, D., Hubacek, K. (2020). "China CO₂ emission accounts 2016-2017." *Scientific Data* 7.
 616 <https://doi.org/10.1038/s41597-020-0393-y>
- 617 Sharma, L.K., Bali, S.K., Dwyer, J.D., Plant, A.B., Bhowmik, A. (2017). "A Case Study of Improving Yield
 618 Prediction and Sulfur Deficiency Detection Using Optical Sensors and Relationship of Historical Potato Yield with
 619 Weather Data in Maine." *Sensors* 17. <https://doi.org/10.3390/s17051095>
- 620 Takeshima, H., Nin-Pratt, A., Diao, X. (2013). "MECHANIZATION AND AGRICULTURAL TECHNOLOGY
 621 EVOLUTION, AGRICULTURAL INTENSIFICATION IN SUB-SAHARAN AFRICA: TYPOLOGY OF
 622 AGRICULTURAL MECHANIZATION IN NIGERIA." *American Journal of Agricultural Economics* 95, 1230-
 623 1236. <https://doi.org/10.1093/ajae/aat045>
- 624 Tatsumi, K., Yamashiki, Y., da Silva, R.V., Takara, K., Matsuoka, Y., Takahashi, K., Maruyama, K., Kawahara, N.
 625 (2011). "Estimation of potential changes in cereals production under climate change scenarios." *Hydrological
 626 Processes* 25, 2715-2725. <https://doi.org/10.1002/hyp.8012>
- 627 Tripathy, R., Chaudhari, K.N., Mukherjee, J., Ray, S.S., Patel, N.K., Panigrahy, S., Parihar, J.S. (2013). "Forecasting
 628 wheat yield in Punjab state of India by combining crop simulation model WOFOST and remotely sensed inputs."
 629 *Remote Sensing Letters* 4, 19-28. <https://doi.org/10.1080/2150704x.2012.683117>
- 630 Urban, D., Roberts, M.J., Schlenker, W., Lobell, D.B. (2012). "Projected temperature changes indicate significant
 631 increase in interannual variability of U.S. maize yields." *Climatic Change* 112, 525-533.
 632 <https://doi.org/10.1007/s10584-012-0428-2>
- 633 van Vuuren, D.P., Carter, T.R. (2014). "Climate and socio-economic scenarios for climate change research and
 634 assessment: reconciling the new with the old." *Climatic Change* 122, 415-429. <https://doi.org/10.1007/s10584-013-0974-2>
- 635 Vancutsem, C., Marinho, E., Kayitakire, F., See, L., Fritz, S. (2013). "Harmonizing and Combining Existing Land
 636 Cover/Land Use Datasets for Cropland Area Monitoring at the African Continental Scale." *Remote Sensing* 5, 19-41.
 637 <https://doi.org/10.3390/rs5010019>
- 638 Vermeulen, S.J., Aggarwal, P.K., Ainslie, A., Angelone, C., Campbell, B.M., Challinor, A.J., Hansen, J.W., Ingram,
 639 J.S.I., Jarvis, A., Kristjanson, P., Lau, C., Nelson, G.C., Thornton, P.K., Wollenberg, E. (2012). "Options for support
 640 to agriculture and food security under climate change." *Environmental Science & Policy* 15, 136-144.
 641 <https://doi.org/10.1016/j.envsci.2011.09.003>
- 642 Wang, Y.-P., Chang, K.-W., Chen, R.-K., Lo, J.-C., Shen, Y. (2010). "Large-area rice yield forecasting using
 643 satellite imageries." *International Journal of Applied Earth Observation and Geoinformation* 12, 27-35.
 644 <https://doi.org/10.1016/j.jag.2009.09.009>
- 645 Wu, T., Yu, R., Zhang, F., Wang, Z., Dong, M., Wang, L., Jin, X., Chen, D., Li, L. (2010). "The Beijing Climate
 646 Center atmospheric general circulation model: description and its performance for the present-day climate." *Climate
 647 Dynamics* 34, 123-147. <https://doi.org/10.1007/s00382-008-0487-2>
- 647 Xie, W., Huang, J., Wang, J., Cui, Q., Robertson, R., Chen, K. (2020). "Climate change impacts on China's
 648 agriculture: The responses from market and trade." *China Economic Review* 62.
 649 <https://doi.org/10.1016/j.chieco.2018.11.007>
- 650 Xinliang, X. (2017a). "Spatially distributed kilometer grid dataset of China's GDP." [Dataset]. *System,
 651 R.a.E.S.D.R.a.P.* <http://www.resdc.cn/DOI/10.12078/2017121102>
- 652 Xinliang, X. (2017b). "Spatially distributed kilometer grid dataset of Chinese population." [Dataset]. *System,
 653 R.a.E.S.D.R.a.P.* <http://www.resdc.cn/DOI/10.12078/2017121101>
- 654 Yang, H., Huang, J., Liu, D. (2020). "Linking climate change and socioeconomic development to urban land use
 655 simulation: Analysis of their concurrent effects on carbon storage." *Applied Geography* 115.
 656 <https://doi.org/10.1016/j.apgeog.2019.102135>
- 657 Yang, Q., Shi, L., Han, J., Zha, Y., Zhu, P. (2019). "Deep convolutional neural networks for rice grain yield
 658 estimation at the ripening stage using UAV-based remotely sensed images." *Field Crops Research* 235, 142-153.
 659 <https://doi.org/10.1016/j.fcr.2019.02.022>
- 660 Yang, X., Lin, E., Ma, S., Ju, H., Guo, L., Xiong, W., Li, Y., Xu, Y. (2007). "Adaptation of agriculture to warming
 661 in Northeast China." *Climatic Change* 84, 45-58. <https://doi.org/10.1007/s10584-007-9265-0>
- 662 Yeldan, O., Colorni, A., Lue, A., Rodaro, E. (2012). "A stochastic continuous cellular automata traffic flow model
 663 with a multi-agent fuzzy system." 15th Meeting of the Euro-Working-Group-on-Transportation (EWGT), Cite
 664 Descartes, Paris, FRANCE, pp. 1350-1359. <https://doi.org/10.1016/j.sbspro.2012.09.849>

- 667 Yin, X.G., Jabloun, M., Olesen, J.E., Ozturk, I., Wang, M., Chen, F. (2016). "Effects of climatic factors, drought
668 risk and irrigation requirement on maize yield in the Northeast Farming Region of China." *Journal of Agricultural
669 Science* 154, 1171-1189. <https://doi.org/10.1017/s0021859616000150>
- 670 Yu, D., Hu, S., Tong, L., Xia, C. (2020). "Spatiotemporal Dynamics of Cultivated Land and Its Influences on Grain
671 Production Potential in Hunan Province, China." *Land* 9. <https://doi.org/10.3390/land9120510>
- 672 Zhang, H., Qi, Y. (2010). "Strategic Thinking on China Low Carbon Economy Development: Taking the Jingjinji
673 Zone as the Example." *China Population·Resources and Environment* 20, 6-11.
- 674 Zhang, P., Yang, Q., Zhao, Y. (2012). "Relationship between social economic agglomeration and labor productivity
675 of core cities in Northeast China." *Chinese Geographical Science* 22, 221-231. [https://doi.org/10.1007/s11769-012-0522-4](https://doi.org/10.1007/s11769-012-
676 0522-4)
- 677 Zhang, Q., Zhang, W., Li, T.T., Sun, W.J., Yu, Y.Q., Wang, G.C. (2017a). "Projective analysis of staple food crop
678 productivity in adaptation to future climate change in China." *International Journal of Biometeorology* 61, 1445-
679 1460. <https://doi.org/10.1007/s00484-017-1322-4>
- 680 Zhang, X., Yang, J., Thomas, R. (2017b). "Mechanization outsourcing clusters and division of labor in Chinese
681 agriculture." *China Economic Review* 43, 184-195. <https://doi.org/10.1016/j.chieco.2017.01.012>
- 682 Zhong, L., Hu, L., Zhou, H. (2019). "Deep learning based multi-temporal crop classification." *Remote Sensing of
683 Environment* 221, 430-443. <https://doi.org/10.1016/j.rse.2018.11.032>
- 684 Zobeidi, T., Yaghoubi, J., Yazdanpanah, M. (2021). "Developing a paradigm model for the analysis of farmers'
685 adaptation to water scarcity." *Environment Development and Sustainability*. [https://doi.org/10.1007/s10668-021-01663-y](https://doi.org/10.1007/s10668-021-
686 01663-y)
- 687 Zongruing, W., Kaishan, S., Xiaoyan, L.I., Bai, Z., Dianwei, L.I.U. (2007). "Effects of Climate Change on Yield of
688 Maize in Maize Zone of Songnen Plain in the Past 40 Years." *Journal of Arid Land Resources and Environment* 21,
689 112-117.
- 690